Core–Corona Particles

DOI: 10.1002/anie.200800331

A Core–Corona Hierarchical Manganese Oxide and its Formation by an Aqueous Soft Chemistry Mechanism**

David Portehault, Sophie Cassaignon, Nadine Nassif, Emmanuel Baudrin, and Jean-Pierre Jolivet*

One of the main challenges that still needs to be overcome in the design of nanotextured materials is the synthesis of uniform complex architectures.[1,2] Indeed, many properties are known to be greatly modified by the size and shape of nanostructures.[1,2] Other than size and shape tailoring, however, control of the ordering between nanostructures and the resulting texture is still difficult. Synthetic routes that make use of organic solvents and templates (i.e., surfactants) often require subsequent purification procedures which significantly increase production costs.[2,3] The development of environmentally friendly, low-cost, and template-free synthetic methods that produce complex architectures is therefore key to enhancing both the control of the properties and the viability of such materials.[4]

In this context, porous manganese oxide materials are attracting great interest due to their applicability in domains such as ion-exchange,[5a] catalysis,[5b] and energy storage in Li batteries and supercapacitors.[5c,d] Indeed, layered birnessite-like manganese oxides (LMO) are particularly relevant due to their lamellar structure, which contain layers of MnO_6 octahedra between which different species can be intercalated (see Figure S1 in the Supporting Information).[5a,b] However, the design of ordered LMO architectures remains a significant challenge[6,7] as their synthesis usually takes place in an aqueous medium by sol–gel or precipitation methods,[6,7] both of which result in fast and uncontrolled solid growth that hinders the synthesis of well-ordered nanostructures.

Herein we present a low-temperature aqueous precipitation of potassium-intercalated LMO with a peculiar hierarchical core–corona architecture in the absence of both a template and an organic medium. Particle formation takes place in an easy "one-pot" process involving two distinct precipitation kinetic stages. The synthesis of similar inorganic/inorganic core–corona morphologies generally requires two steps for core formation and shell growth,[8] and there are very few reports concerning one-pot procedures that lead to fully inorganic core–shell particles.[9] Furthermore, these methods are generally limited to metal–oxide structures. The approach presented herein, which uses in situ seeding to control the solid growth, significantly broadens the range of strategies available for the elaboration of hierarchical inorganic structures and can be extended to the design of new functional nanostructured materials, by taking advantage of the unique oxide properties, in areas such as catalysis, energy harnessing, and information storage.

The synthesis of birnessite (see the Experimental Section and the Supporting Information) is based on the redox reaction between $MnSO_4$ and an excess of $KMnO_4$[4f,5b] (total Mn concentration of $0.2\,mol\,L^{-1}$) in water according to Equation (1). Mixing the acidic (pH 2) solutions of the

$$2\,MnO_4^- + 3\,Mn^{2+} + 2\,H_2O \rightarrow 5\,MnO_2 + 4\,H^+ \quad (1)$$

soluble precursors at room temperature led immediately to a black precipitate and the mixture was then heated at 95 °C for between one and seven days. The resulting powder was collected by centrifugation, washed several times with water, and dried at room temperature. The procedure gave a quantitative yield of product (approx. 4 g).

The powder X-ray diffraction (XRD) patterns (Figure 1) clearly show that the initial precipitate is poorly ordered. Phase ordering occurs upon aging at 95 °C, however, and the characteristic peaks (JCPDS file no. 80-1098) of K-birnessite-type LMO (b-LMO) appear after 2 h. The composition of this compound, as evaluated by elemental analysis and average

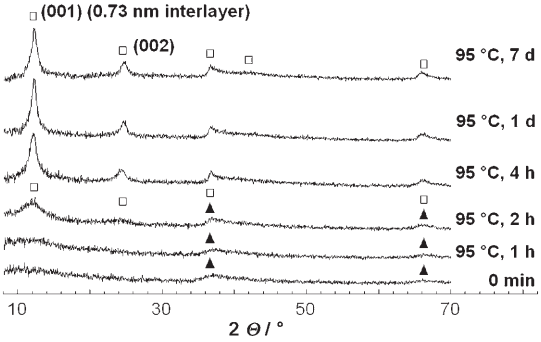

Figure 1. Powder XRD patterns after different times of aging at 95 °C. Disordered early precipitate (▲) and birnessite layered manganese oxide (b-LMO) (□).

[*] D. Portehault, Dr. S. Cassaignon, Dr. N. Nassif, Prof. J.-P. Jolivet
Chimie de la Matière Condensée de Paris
UMR CNRS 7574, UPMC-Paris6
cc 174, 4 place Jussieu, 75005 Paris (France)
Fax: (+33) 1-4427-4769
E-mail: cassai@ccr.jussieu.fr
Dr. E. Baudrin
Laboratoire de Réactivité et Chimie des Solides
UMR CNRS 6007
Université de Picardie–Jules Verne, Amiens (France)

[**] The authors acknowledge Sophia Khan for experimental support, Dr. Patricia Beaunier (University of Paris 6) for TEM measurements, Annie Richard and Dominique Jalabert (University of Orléans) for FESEM and HRTEM measurements, and Anny Anglo (University of Paris 6) for performing the ultrathin sections.

Supporting information for this article is available on the WWW under http://dx.doi.org/10.1002/anie.200800331.

oxidation state titration, is $K_{0.19}MnO_{1.77}(H_2O)_{0.30}$. A careful examination of the XRD patterns reveals similarities between the early disordered solid and the final birnessite: the only peaks that are missing for the early precipitate are (00l) harmonics, which suggests that the poorly ordered solid already contains sheets of MnO_6 octahedra but that they are not oriented with respect to each other.

The morphology of samples after different stages of evolution was examined by field-emission scanning electron microscopy (FESEM). Low magnification showed that a unique morphology was obtained (Figures S2 and S3 in the Supporting Information), with ball-like particles with an average diameter of less than 100 nm being observed immediately after mixing (Figure 2a). Elemental analysis

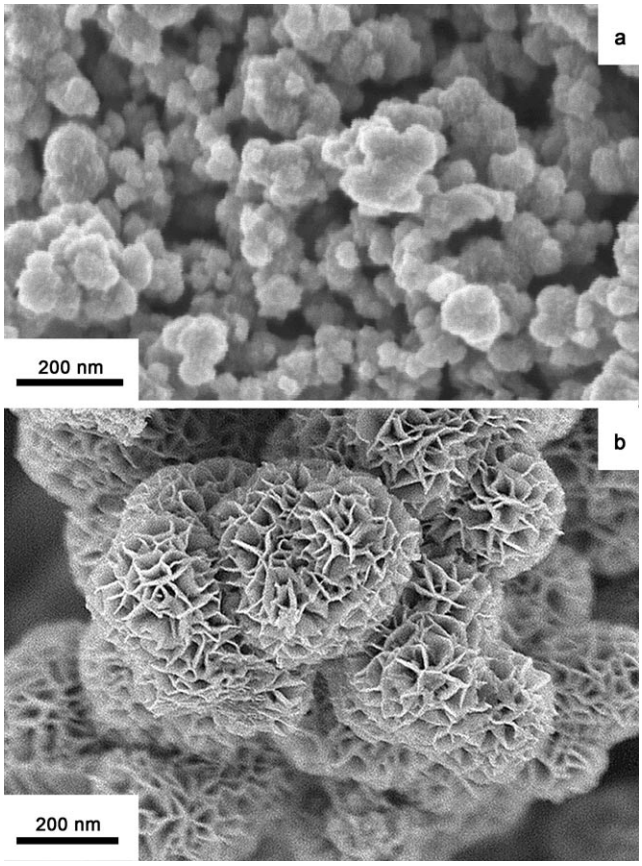

Figure 2. FESEM images of the early precipitate (a) and of b-LMO obtained after aging for one day at 95 °C (b).

indicated that the early precipitate contained around 3 mol % K^+, in agreement with the mean calculated Mn oxidation state (3.99). After aging for one day the particle diameter had increased to around 400 nm (Figure 2b). This material is nanotextured and exhibits a peculiar spongelike architecture, with percolated radial walls with a thickness of approximately 10 nm. This value is in agreement with that determined with the Scherrer formula from the broadening of the (001) XRD peak. EDX confirmed that b-LMO contains larger amounts of potassium than the early precipitate (Figure S4 in the Supporting Information).

Transmission electron microscopy (TEM) revealed the uniform "crumpled paper ball" morphology of the early solid, while selected-area electron diffraction (SAED) confirmed that it is poorly ordered (Figure 3a). The characteristic

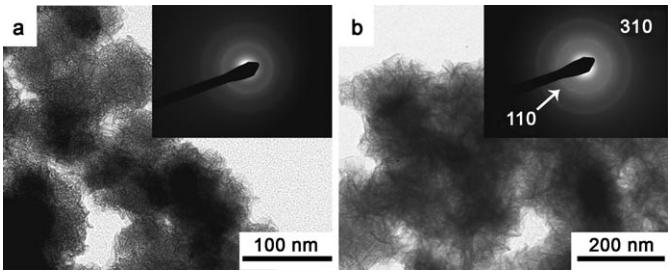

Figure 3. TEM images and the corresponding SAED patterns (insets) of the disordered early precipitate (a) and of b-LMO obtained after aging for one day at 95 °C (b).

distances of the b-LMO structure, although without preferential orientation of the crystallites, could be seen after one day of aging (Figure 3b (inset)). Interestingly, TEM performed at this stage on ultrathin sections of an embedded sample revealed a core–corona architecture (Figure 4) where the 200-nm-diameter core is denser than the corona. Further high resolution TEM (HRTEM) experiments showed that this core is poorly ordered (Figure 4) and thus retains the character of the early precipitate particles. However, HRTEM also indicated that the corona (thickness of around 100 nm) is made of thin radial walls crystallized in the birnessite structure, with MnO_6 layers in a radial orientation. The d-spacing of around 0.61 nm is consistent with the spacing between the (001) planes, which are dehydrated under the electron beam. Similar investigations on the material obtained after aging for seven days indicated an increase in

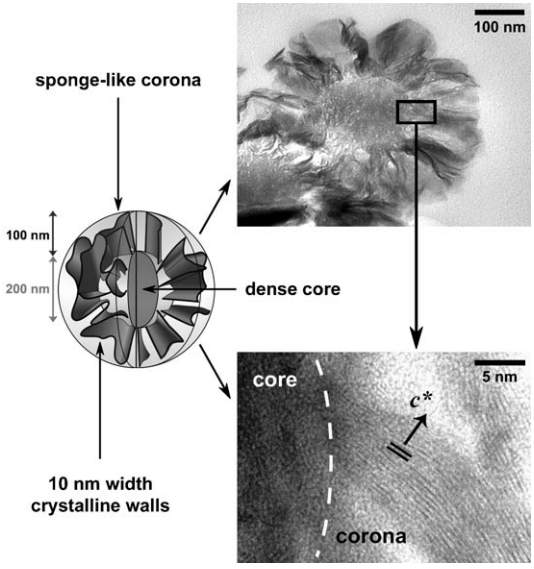

Figure 4. Right: TEM and HRTEM images of ultrathin sections of b-LMO with a core–corona architecture after aging for one day. Left: schematic drawing of a core–corona b-LMO particle with a poorly organized core and crystalline corona.

the final particle diameter (Figure S3 in the Supporting Information).

The results of a supernatant titration (see the Supporting Information) performed to follow the reactant consumption[4f] indicated that Mn^{2+} had reacted completely after one hour. After 1 day of aging, 70% of the initial quantity of $KMnO_4$ had been consumed and a strong pH increase (pH of around 12) was observed. This pH increase and the MnO_4^- consumption, which is higher than that expected from the reaction in Equation (1) (18%), indicate that a secondary reaction involving slow oxidation of water by the excess MnO_4^- takes place [Eq. (2)]. Slow precipitation of manganese oxide is therefore accompanied by strong proton consumption.

$$4\,MnO_4^- + 4\,H^+ \rightarrow 4\,MnO_2 + 3\,O_2 + 2\,H_2O \qquad (2)$$

These results enable us to propose a formation mechanism for this ordered architecture (Scheme 1). The initial reaction between MnO_4^- and Mn^{2+} ions is too fast to enable

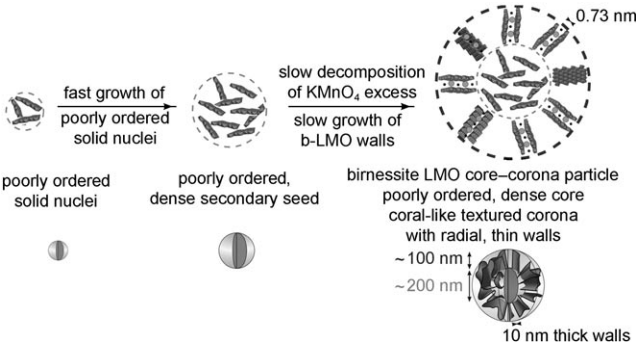

Scheme 1. Proposed reaction scheme for the formation of core–corona particles of birnessite layered manganese oxide (b-LMO). ○ and ● represent interlamellar K^+ and H_2O species, respectively.

orientation between the sheets of octahedra and leads to small, poorly ordered, ball-like particles. Fast growth of the nuclei then occurs. As Mn species have a very low solubility in the alkaline aging medium in the absence of a complexant the early precipitate particles do not dissolve and therefore conserve their shape and disordered structure. In the second stage, these kinetically stable initial particles act as seeds for decomposition of the excess MnO_4^-, which is slower than the reaction in Equation (1). Thus, the slow precipitation that occurs around the seeds enables the oriented growth of an architecture consisting of high, thin crystalline walls due to the two-dimensional lamellar structure of b-LMO. Similar spongelike morphologies of layered manganese oxides have been reported,[7b,d] although as their syntheses involve decomposition of a single precursor ($KMnO_4$ or a cyclen–manganese complex) there can be only one kinetic pathway, thus hindering the formation of core–corona architectures. Interestingly, the one-pot, two-step process developed herein can be applied to the previously reported synthesis of other oxide–oxide[4e] or metal–oxide[9e] particles involving a catalyzed fast initial step for core formation and a second, slower stage for shell growth. Additionally, Liz-Marzán's group has reported the formation of Ag–TiO_2 particles upon directly mixing Ag^I and Ti^{IV} precursors under reducing conditions in the presence of a strong Ti^{IV} complexant.[9b] Precipitation of the Ag core occurred upon fast reduction, while the chelating agent slowed the hydrolysis of Ti^{IV} and led to the formation of a TiO_2 shell. Such procedures involving two kinetic pathways show the great potential of our approach for the design of core–corona architectures.

In summary, hierarchical 3D architectures can be synthesized by a simple one-pot method free of any organic additives, which involves aqueous precipitation at low temperature. The formation of uniform core–corona particles occurs in two distinct precipitation steps: the first, fast stage involves in situ seeding while the second step involves a slow reaction for oriented growth. This synthetic route towards elaborate architectures brings out new aspects of metal oxide crystallization and is currently being investigated for application to various compounds. The hierarchical textured corona of these particles could greatly enhance the exchange and electrochemical properties of the material.

Experimental Section

Nitrogen was bubbled through an aqueous solution of $MnSO_4{\cdot}H_2O$ (30 mL, 6.5 mmol) for 30 min then the pH was adjusted to 2 by addition of a 2 M H_2SO_4 solution. A $KMnO_4$ solution (200 mL, 43 mmol; pH 2) was added whilst stirring and the volume was adjusted to 250 mL by adding a pH 2 aqueous solution of H_2SO_4. The suspensions were aged at 95 °C and shaken once per day. Samples were collected at different times over seven days and centrifuged. The powders were washed three times with deionized water and dried at room temperature under a nitrogen flow. Characterization of the solid was performed by elemental analysis, oxidation state titration, XRD ($Cu_{K\alpha}$), FESEM (2 kV) and EDX, TEM (100 and 200 kV), and SAED. Titration of Mn^{2+} and MnO_4^- in the aging medium was performed by an electrochemical method. Experimental details are given in the Supporting Information, together with the structure of b-LMO, low magnification FESEM images, EDX spectra, FESEM images of truncated particles, TEM performed on an ultrathin section of the initial precipitate, and an HRTEM image of an uncut particle.

Received: January 22, 2008
Revised: May 7, 2008
Published online: July 10, 2008

Keywords: crystal growth · layered compounds · manganese · nanostructures · synthesis design

[1] a) A. P. Alivisatos, *Science* **1996**, *271*, 933–937; b) A. Bezryadin, C. N. Lau, M. Tinkham, *Nature* **2000**, *404*, 971–974.
[2] a) L. Manna, D. J. Milliron, A. Meisel, E. C. Scher, A. P. Alivisatos, *Nat. Mater.* **2003**, *2*, 382–385; b) H. Cölfen, M. Antonietti, *Angew. Chem.* **2005**, *117*, 5714–5730; *Angew. Chem. Int. Ed.* **2005**, *44*, 5576–5591.
[3] Z. R. Tian, J. A. Voigt, J. Liu, B. McKenzie, M. McDermott, M. A. Rodrigez, H. Konishi, H. Xu, *Nat. Mater.* **2003**, *2*, 821–826.
[4] a) R. L. Penn, J. F. Banfield, *Geochim. Cosmochim. Acta* **1999**, *63*, 1549–1557; b) B. Liu, H. C. Zeng, *J. Am. Chem. Soc.* **2004**, *126*, 8124–8125; c) J. Yuan, W.-N. Li, S. Gomez, S. L. Suib, *J. Am. Chem. Soc.* **2005**, *127*, 14184–14185; d) Y. Zheng, Y. Cheng, F. Bao, Y. Wang, Y. Qin, *J. Cryst. Growth* **2006**, *286*, 156–161; e) Z.

Li, Y. Ding, Y. Xiong, Q. Yang, Y. Xie, *Chem. Commun.* **2005**, 918 – 920; f) D. Portehault, S. Cassaignon, E. Baudrin, J.-P. Jolivet, *Chem. Mater.* **2007**, *19*, 5410 – 5417.

[5] a) O. Prieto, M. D. Arco, V. Rives, *J. Mater. Sci.* **2003**, *38*, 2815 – 2824; b) S. L. Suib, *Curr. Opin. Solid State Chem.* **1998**, *3*, 63 – 70; c) S. Bach, J. P. Pereira-Ramos, N. Baffier, *J. Solid State Chem.* **1995**, *120*, 70 – 73; d) T. Brousse, M. Toupin, R. Dugas, L. Athouel, O. Crosnier, D. Belanger, *J. Electrochem. Soc.* **2006**, *153*, A2171 – A2180.

[6] a) J. Luo, A. Huang, S. H. Park, S. L. Suib, C.-L. O'Young, *Chem. Mater.* **1998**, *10*, 1561 – 1568; b) S. Ching, D. J. Petrovay, M. L. Jorgensen, S. L. Suib, *Inorg. Chem.* **1997**, *36*, 883 – 890.

[7] a) Y. Oaki, H. Imai, *Angew. Chem.* **2007**, *119*, 5039 – 5043; *Angew. Chem. Int. Ed.* **2007**, *46*, 4951 – 4955; b) D. Yan, P. X. Yan, G. H. Yue, J. Z. Liu, J. B. Chang, Q. Yang, D. M. Qu, Z. R. Geng, J. T. Chen, G. A. Zhang, R. F. Zhuo, *Chem. Phys. Lett.* **2007**, *440*, 134 – 138; c) J. Ge, L. Zhuo, F. Yang, B. Tang, L. Wu, C. Tung, *J. Phys. Chem. B* **2006**, *110*, 17854 – 17859; d) J. P. Hill, S. Alam, K. Ariga, C. E. Anson, A. K. Powell, *Chem. Commun.* **2008**, 383 – 385; e) O. Giraldo, J. P. Durand, H. Ramanan, K. Laubernds, S. L. Suib, M. Tsapatis, S. L. Brock, M. Marquez, *Angew. Chem.* **2003**, *115*, 3011 – 3015; *Angew. Chem. Int. Ed.* **2003**, *42*, 2905 – 2909.

[8] L. Liz-Marzán, P. Mulvaney, *J. Phys. Chem. B* **2003**, *107*, 7312 – 7326.

[9] a) C. N. R. Rao, S. R. C. Vivekchand, K. Biswas, A. Govindaraj, *Dalton Trans.* **2007**, 3728 – 3749; b) I. Pastoriza-Santos, D. S. Koktysh, A. A. Mamedov, M. Giersig, N. A. Kotov, L. Liz-Marzán, *Langmuir* **2000**, *16*, 2731 – 2735; c) R. T. Tom, A. S. Nair, N. Singh, M. Aslam, C. L. Nagendra, R. Philip, K. Vijayamohanan, T. Pradeep, *Langmuir* **2003**, *19*, 3439 – 3445; d) X. M. Sun, Y. D. Li, *Langmuir* **2005**, *21*, 6019 – 6024; e) J. Lai, K. V. P. M. Shafi, A. Ulman, K. Loos, R. Popovitz-Biro, Y. Lee, T. Vogt, C. Estournes, *J. Am. Chem. Soc.* **2005**, *127*, 5730 – 5731; f) J. Du, J. Zhang, Z. Liu, B. Han, T. Jiang, Y. Huang, *Langmuir* **2006**, *22*, 1307 – 1312.

